Available online at www.sciencedirect.com
ScienceDirect
Journal of Theoretical Biology 250 (2008) 424–434
Journal of Theoretical Biology
www.elsevier.com/locate/yjtbi

From individual to collective displacements in heterogeneous environments

E. Casellas[a], J. Gautrais[a], R. Fournier[b], S. Blanco[b], M. Combe[a], V. Fourcassié[a], G. Theraulaz[a], C. Jost[a,*]

[a]*Centre de Recherches sur la Cognition Animale, CNRS-UMR, Université Paul Sabatier, Bât IVR3, 31062 Toulouse cedex 9, France*
[b]*Laboratoire Plasma et Conversion d'Energie, CNRS-UMR, Université Paul Sabatier, 31062 Toulouse cedex 9, France*

Received 26 March 2007; received in revised form 2 October 2007; accepted 10 October 2007
Available online 23 October 2007

Abstract

Animal displacement plays a central role in many ecological questions. It can be interpreted as a combination of components that only depend on the animal (for example a random walk) and external influences given by the heterogeneity of the environment. Here we treat the case where animals switch between random walks in a homogeneous 2D environment and its 1D boundary, combined with a tendency for wall-following behaviour (thigmotactism) that is treated as a Markovian process. In the first part we use mesoscopic techniques to derive from these assumptions a set of partial differential equations (PDE) with specific boundary conditions and parameters that are directly given by the individual displacement parameters. All assumptions and approximations made during this derivation are rigorously validated for the case of exploratory behaviour of the ant *Messor sanctus*. These PDE predict that the stationary density ratio between the 2D (centre) and 1D (border) environment only depends on the thigmotactic component, not on the size of the centre or border areas. In the second part we test this prediction with the same exploratory behaviour of *M. sanctus*, in particular when many ants move around simultaneously and may interact directly or indirectly. The prediction holds when there is a low degree of heterogeneity (simple square arena with straight borders), the collective behaviour is "simply" the sum of the individual behaviours. But this prediction breaks down when heterogeneity increases (obstacles inside the arena) due to the emergence of pheromone trails. Our approach may be applied to study the effects of animal displacement in any environment where the animals are confronted with an alternation of 2D space and 1D borders as for example in fragmented landscapes.

Keywords: Wall-following behaviour; Thigmotactism; Animal displacement; Random walk; Ants

1. Introduction

Animal displacement in space is a basic ingredient of many questions arising in the context of ecology and behavioural ecology (Parrish and Hamner, 1997; Turchin, 1998), in particular when trying to understand spatial patterns such as clustering (Theraulaz et al., 2002; Jeanson et al., 2005; Jost et al., 2007). A detailed understanding of the role of displacement often requires mathematical modelling. The most intuitive approach is a Lagrangian or individual based model (IBM, Grimm and Railsback, 2005) that can readily be parameterized from observed individual trajectories. However, IBM's are computer intensive, especially when many individuals are involved. In such cases, Eulerian models that focus on animal densities, such as (partial) differential equations (PDE, of the reaction–diffusion type), become more efficient tools and they are accessible to analytical study. The parameters of a PDE can in simple cases be deduced from individual trajectories, see Appendix A and Patlak (1953), Kareiva and Shigesada (1983) or Benhamou (2004).

Individual animal displacement in a homogeneous space can frequently be modelled as a correlated random walk (Bovet and Benhamou, 1988; Turchin, 1998; Challet et al., 2005). Such a random walk corresponds at the population level to a diffusive process with a diffusion coefficient that can be estimated from the animal's movement

*Corresponding author. Tel.: +33 561 55 64 37; fax: +33 561 55 61 54.
E-mail address: jost@cict.fr (C. Jost).

0022-5193/$ - see front matter © 2007 Elsevier Ltd. All rights reserved.
doi:10.1016/j.jtbi.2007.10.011

characteristics (Patlak, 1953; Challet et al., 2005) or from its net squared displacement (Einstein, 1905; Kareiva and Shigesada, 1983). In the presence of simple heterogeneities such as well defined borders, the random walk model may no longer apply since displacement often corresponds to a thigmotactic behaviour (Fraenkel and Gunn, 1961, thigmo = 'touch'), that is a tendency to align with a border and move along it for some time. Borders may also separate two habitats (Fagan et al., 1999; Ovaskainen and Cornell, 2003) where animals follow the border and then choose randomly one or the other habitat. The times moving along a border may depend on the border curvature (Creed and Miller, 1990) and they are often exponentially distributed (Sikora et al., 1992; Jeanson et al., 2003), which indicates that the rate to leave the border is constant in time.

In the first part of this paper we will start with an IBM approach to model the movement of animals in 2D space with borders (or edges) of different curvature. The underlying hypotheses of this IBM will be validated with experimental trajectories of exploring *Messor sanctus* ants. We will then develop a PDE model that is directly linked to the characteristics of individual trajectories, in particular those describing the random walk and wall-following behaviours. Furthermore, we will validate experimentally and by numerical simulations all the approximations that occur when passing from the IBM to the PDE model. This rigorously validated model will serve in future work to understand more complex spatial phenomena such as object clustering (Theraulaz et al., 2002) and its coupling with external factors such as temperature (Challet et al., 2005) or air currents (Jost et al., 2007).

The approach used by Patlak (1953) and in this paper implicitly assumes that animals move the same independently of whether they are alone or whether there are conspecifics around. This is a strong assumption, in particular for social insects that are known to exhibit social interactions leading to collective movement along well-defined recruitment trails (Camazine et al., 2001). In the second part we therefore test experimentally (exploratory behaviour of *M. sanctus* ants) whether displacement at the collective level corresponds to the sum of individual displacements or whether something new emerges from the interactions between individuals. Our test is based on the model prediction that at stationary state the mean border following time should determine the ratio of ant densities in the central and border zones (Section 2).

2. The model and its predictions at stationary state

We consider ant displacement in an arena with a 2D central zone and a 1D border zone. Let us denote by $n_c(x,y,t)$ the (2D) ant density at coordinates (x,y) at time t, and by $n_b(\sigma,t)$ the (1D) density at the (linear) position σ along the border at time t. In the central zone ants move with a standard 2D diffusive random walk. This corresponds at the macroscopic level to a diffusion equation

$$\frac{\partial n_c}{\partial t} = -\mathbf{div}(-D_c\,\mathbf{grad}\,n_c) = -\mathbf{div}(\vec{j}),$$

where **div** denotes divergence, $\vec{j} = -D_c\,\mathbf{grad}\,n_c$ is the flux density vector and D_c is the diffusion coefficient computed from the random walk parameters (see Appendix A and Patlak, 1953 for further details). If D_c is constant in space it can be extracted from the divergence term, leading to the more familiar equation

$$\frac{\partial n_c}{\partial t} = D_c\,\mathbf{div}(\mathbf{grad}\,n_c) = D_c\Delta n_c \tag{1}$$

with $\Delta = \partial^2/\partial x^2 + \partial^2/\partial y^2$. Note that we use here the most simple case of Fickian diffusion, but the reasoning below at stationary state would also hold for other diffusion models such as the Fokker–Planck or the telegraph equation.

Ants that move along the arena wall make U-turns at a constant rate and thus also do a (1D) random walk. At the macroscopic level the dynamics of n_b can thus be described as in Eq. (1), with the diffusion coefficient D_b.

We now have to add to the model the passages from the centre to the border and back. In order to formulate these passages in terms of the underlying animal behaviour we cannot reason on the density level (macroscopic) without stating explicitly the statistics of the underlying directional propagation (mesoscopic) on the basis of corpuscular transport theory (Case and Zweifel, 1967), a technique that was also used by Patlak (1953) or more recently by Grünbaum (1999) and Faugeras and Maury (2007). In the present case we have to consider the density of ants at point (x,y) that walk in direction $\vec{u}$, the phase space density $f(x,y,\vec{u},t)$. By definition (see Appendix A) we have $n_c(x,y,t) = \int_{\vec{u}} f(x,y,\vec{u},t)\,\mathrm{d}\vec{u}$ and $\vec{j}(x,y,t) = \int_{\vec{u}} v_c f(x,y,\vec{u},t)\vec{u}\,\mathrm{d}\vec{u}$ (where v_c is the ant speed in the central zone). When establishing Eq. (1) on the basis of the observed statistical behaviours (Appendix A), the so-called $P1$ approximation is used for the angular dependance of f:

$$f(x,y,\vec{u},t) \approx a n_c(x,y,t) + b\vec{j}\cdot\vec{u}, \tag{2}$$

where a and b are constant values. In two dimensions, this corresponds to the first two terms of a Fourier series, with $a = 1/(2\pi)$ and $b = 1/(\pi v_c)$. The total flux density from the centre to the border through a particular point along the border is now computed by integrating over all $\vec{u}$:

$$\begin{aligned} & v_c \int_{\mathbf{centre}\to\mathbf{border}} \vec{u}\cdot\vec{n} f(x,y,\vec{u},t)\,\mathrm{d}\vec{u} \\ & \overset{(2)}{\approx} v_c \frac{n_c}{2\pi}\int_{-\pi/2}^{\pi/2} \cos\gamma\,\mathrm{d}\gamma \\ & \quad + \frac{1}{\pi}\int_{-\pi/2}^{\pi/2}\left(\begin{pmatrix}\cos\gamma\\ \sin\gamma\end{pmatrix}\cdot\vec{n}\right)\left(\vec{j}\cdot\begin{pmatrix}\cos\gamma\\ \sin\gamma\end{pmatrix}\right)\mathrm{d}\gamma \\ & = v_c\frac{n_c(x,y,t)}{\pi} + \frac{1}{2}\vec{j}\cdot\vec{n}, \end{aligned}$$

where $\vec{n}$ is the (outward) normal vector to the border segment and γ is the angle between $\vec{u}$ and $\vec{n}$.

The passage from the border back to the centre of the arena is given by the rate at which ants quit the border. If we assume that this rate is Markovian and constant for borders with fixed curvature then this rate is simply the inverse of the mean border following distance before returning to the central zone ($1/\lambda_b$). Denoting by v_b the animal speed along the border we get the flux density

$$n_b(\sigma,t)\frac{v_b}{\lambda_b}.$$

Combining all these equations we get the macroscopic equations

$$\frac{\partial n_c}{\partial t} = D_c \Delta n_c, \tag{3}$$

$$\frac{\partial n_b}{\partial t} = D_b \Delta n_b + n_c \frac{v_c}{\pi} + \frac{1}{2}\vec{j}\cdot\vec{n} - n_b \frac{v_b}{\lambda_b},$$

$$\vec{j}\cdot\vec{n} = n_c \frac{v_c}{\pi} + \frac{1}{2}\vec{j}\cdot\vec{n} - n_b \frac{v_b}{\lambda_b} \quad \text{boundary conditions},$$

where the last two equations simplify to

$$\frac{\partial n_b}{\partial t} = D_b \Delta n_b + 2\left(n_c \frac{v_c}{\pi} - n_b \frac{v_b}{\lambda_b}\right), \tag{4}$$

$$\vec{j}\cdot\vec{n} = 2\left(n_c \frac{v_c}{\pi} - n_b \frac{v_b}{\lambda_b}\right) \quad \text{boundary conditions} \tag{5}$$

and Eq. (5) represents the boundary conditions for Eq. (3) in terms of flux density $\vec{j}\cdot\vec{n}$ with the normal vector $\vec{n}$ pointing outward. Eq. (4) has circular boundary conditions (the arena border is closed). Note that the boundary conditions (5) are unusual in traditional models of animal movement that most often use reflecting boundaries ($\vec{j}\cdot\vec{n} = 0$) or absorbing boundaries ($n_c = n_0$, a fixed value along the border), see Turchin (1998) or Okubo and Levin (2001, p. 301) for short summaries. For quantitative predictions with this model we will perform numerical simulations based on a time integration scheme (Euler scheme) and a centred finite difference scheme for the spatial integration (Press et al., 1992, p. 487).

At stationary state the fluxes to and from the border are the same, that is

$$n_c^s \frac{v_c}{\pi} = n_b^s \frac{v_b}{\lambda_b} \overset{v_b = v_c}{\Rightarrow} \frac{n_c^s}{\pi} = \frac{n_b^s}{\lambda_b}, \tag{6}$$

where the superscript s indicates densities at stationary state and where we further assume ant speed to be the same in the centre and along the border. This reasoning can be extended easily to account for two types of borders, for example straight borders (walls, with linear density n_w and mean free path λ_w) and concave borders (for example circular obstacles, n_b and λ_b, see Fig. 5). We then get the relations

$$\lambda_b = \pi \frac{n_b^s}{n_c^s} \quad \text{and} \quad \lambda_w = \pi \frac{n_w^s}{n_c^s}. \tag{7}$$

These relations permit to validate the model predictions at stationary state. We only have to estimate the mean densities in the centre and the different border areas of the arena once the system has reached its stationary state to compute the predicted λ_b and λ_w. These values can then be compared with the mean border following distances measured on individual ants.

Note that predictions (7) hold because our ants move at the same speed $v = v_b = v_c$ in the centre and along the borders. If they were to move at different speeds then v would not cancel out in Eq. (6) and the speeds would be part of the predicted density ratios in Eq. (7).

3. Estimating individual displacement parameters and validating model hypotheses

Experiments were performed with a colony of the Mediterranean seed-harvesting ant *M. sanctus* Emery (Myrmicinae). All experiments were done in a closed chamber of size $35 \times 35 \times 30$ cm (length, width, height) whose walls and floor were painted white and which was covered by a transparent acrylic glass. Since temperature influences ant displacement (Challet et al., 2005) we controlled it through circulating water set at a constant temperature (23 °C) in the chamber floor and walls (Jost et al., 2007). Outside temperature was set to ≈ 24 °C to ensure that the temperature of the acrylic glass covering the chamber did not create any convective air currents. The ant colony was placed beneath the closed chamber and ants had access to the chamber floor (subsequently called arena) freely by climbing along a small wooden stick through a hole in the centre of the arena (see Jost et al., 2007 for further details). Access to this wooden stick could experimentally be interrupted to control the number of ants in the arena. Ant displacement was then filmed through the acrylic glass (Sony digital camera DCR-VX2000E). The arena was either empty, containing three circular obstacles (6 cm diameter, curvature $\frac{1}{3}\,\text{cm}^{-1}$), seven obstacles (4 cm, $\frac{1}{2}\,\text{cm}^{-1}$) or 10 obstacles (2 cm, $1\,\text{cm}^{-1}$), see Fig. 5. For the obstacles we chose white cylinders of height 1 cm that were coated with Fluon© in order to prevent the ants from mounting on them.

In a first series of experiments we had to confirm that *M. sanctus* ants move indeed with diffusive random walks. Individual animal displacement was analysed in two parts of the arena: the border zone (that consists of a 1 cm wide strip along the border of walls or obstacles) and the central zone. One cm corresponds approximately to the distance over which a *M. sanctus* ant can detect conspecifics or the obstacles that we used (Fourcassié et al., 2003). To analyse displacement in the central zone, an ant was given access to the arena and filmed during 1 min or until it hit the arena wall. Its path was then digitized with Ethovision (version 3.0, Noldus Information Technology) at the rate of two points per second. Seventy-seven paths were obtained and analysed to extract the random walk parameters (Turchin, 1998; Challet et al., 2005). Computing the net squared displacement from these paths will permit to validate the non-stationary (diffusive) dynamics in the central zone (Einstein, 1905). This is technically equivalent to say that

the $P1$-approximation made when deriving the PDE (Appendix A) holds. The diffusion coefficient D_c could be computed from the slope of the net squared displacement curve (Kareiva and Shigesada, 1983), but in analogy with the mesoscopic reasoning in Appendix A we will estimate it from the behavioural displacement parameters. Each path was decomposed into a sequence of straight moves (free paths) and turning angles between moves (see Challet et al., 2005 for details). Since for technical reasons moves have a minimal length (here 1 cm to remove artificial moves due to digitization noise, Tourtellot et al., 1991) the mean move length or mean free path l was not simply estimated as the mean of the moves (which would be positively biased) but as the inverse of the survival curve slope on log-linear scale, obtained with weighted linear regression where the weights are the standard errors around the survival curve (Haccou and Meelis, 1992). This procedure also permits to test whether the survival curve follows an exponential distribution (Haccou and Meelis, 1992, p. 144). The distribution of the turning angles was tested for symmetry (Zar, 1999, p. 115) and its shape quantified by the mean cosine g (which is close to 1 for forward oriented paths, 0 for uniformly distributed turning angles and close to -1 when there is a high tendency for U-turns; see Appendix A for a formal definition). Free paths and turning angles were also tested for autocorrelation. Finally, the speed v was estimated as the total path length divided by the recording time. The mean values ($\pm$ se) of the parameters l, g, and v were computed from the 77 paths. This allowed us to compute the diffusion coefficient $D_c = vl/(2(1-g))$ used in Eq. (3) (see Appendix A). The diffusion coefficient corresponding to border following behaviour D_b can be estimated similarly as $D_b = v^2/(2/\tau_b + 1/\tau_q)$ with τ_b and τ_q being the mean time walked along the border before making a U-turn or leaving the border, respectively (see Appendix A for more theoretical background).

To analyse border following behaviour 30–40 ants were allowed to enter the arena (before interrupting the access with the wooden stick) and their displacement was filmed continuously. This procedure was used to increase the number of border following events. When an ant entered the 1 cm wide strip along the arena walls or obstacle borders and remained there for at least 2 s (to ensure that it was indeed in the border following behavioural mode) we measured the total time before the ant leaves the border or makes a U-turn (at most the first 10 events were taken per obstacle to reduce any potential effect of chemical marking). We only took into account events during which ants had no contact with conspecifics. These times were also analysed as survival curves to estimate the mean time an ant follows a border. The standard error of this mean time was estimated with a non-parametric bootstrap. A Kruskal–Wallis test was used to compare the times of the different obstacle diameters. The mean border following distances λ (see Section 2) were obtained by multiplying the mean times by the mean speed v.

3.1. Estimating ant densities in the arena

To estimate the average ant densities in the centre and border zone 30–40 ants were given access to the arena. After 30 min (to let these ants reach a stationary distribution, see Fig. 4) the whole arena was filmed for 90 min. This film was analysed at 1 frame per second in order to get an estimate of the mean density over the arena during this duration.

First a mask was fitted in order to exclude from the analysis all obstacle surfaces and a zone of 1 cm around the central entry hole. Then a grey level threshold was calibrated by eye to distinguish pixels belonging to ants (above the threshold) from the pixels of the background. The mean frequency of ants on a pixel was estimated as the number of frames an ant was detected on this pixel, divided

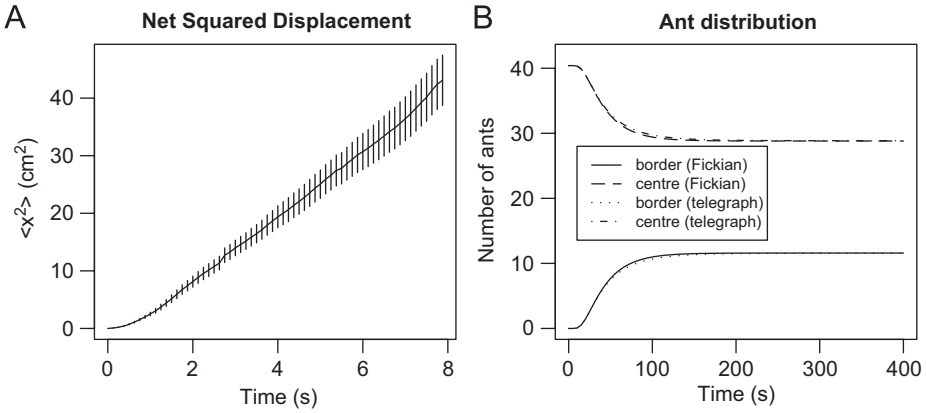

Fig. 1. Validation of non-stationary dynamics. (A) Net squared displacement (mean $\pm$se, $n = 55$) of ants in the arena centre as a function of time. After a short ballistic phase (1–2 s) the curve increases linearly with time. (B) Numerical simulation of the temporal dynamics of the number of ants in the centre or along the border. They show that there is barely a difference between pure Fickian diffusion everywhere or the telegraph equation along the border with Fickian diffusion in the centre (100 by 100 square grid with $dx = dy = 0.0035$ m, $dt = 0.002$ s and the parameters as given in the results section; the numerical solutions were tested for independence of the particular temporal and spatial discretization).

by the total number of analysed frames. These frequencies were then summed over all pixels belonging either to the central zone, the wall border zone or the obstacle border zone. Dividing these sums by the total surface of the central zone or the length of the 1 cm wide bands along the borders finally gave a relative measure of ant density in these zones during the 90 min observation time. The fraction of border density by the centre density (multiplied by π and divided by mean ant speed v, see Section 2) gave the predicted mean border following time.

During the image analysis some pixels turned out to be above the threshold almost throughout the whole 90 min without any ants on them (mostly 'shaded' pixels close to the wall or obstacles). There was no way to identify these pixels unambiguously. Therefore we removed from the density analysis 5–10% of the densest pixels, giving a range of estimates for the border following times. Since this range has no statistical meaning such as a standard error, we compared these ranges only qualitatively to the measured border following times.

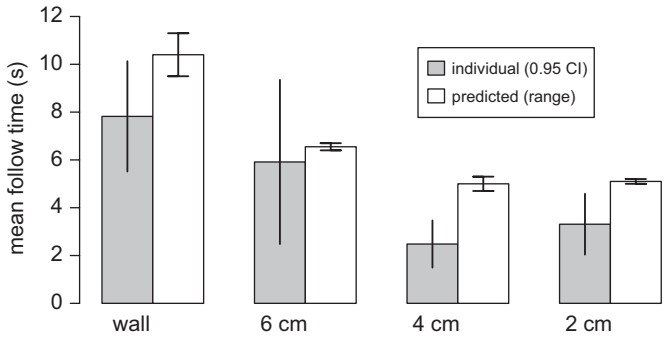

Fig. 2. Mean border following times estimated from the individual paths (grey bars, with 95% confidence interval CI) and ranges of predicted times calculated from the density estimates (white bars), for walls, large (6 cm diameter), median (4 cm) and small obstacles (2 cm).

4. Results

Ants walked with a mean speed of $v = 1.40 \pm 0.04$ cm/s (mean $\pm$ se). Comparison between ant speeds in the centre and along the border showed no difference ($F_{1,28} = 1.76$, $p = 0.195$). The paths had non-correlated exponentially distributed free paths with mean free path $l = 0.77 \pm 0.04$ cm and non-correlated turning angles with a symmetric distribution and a mean asymmetry coefficient $g = 0.62 \pm 0.01$. These values result in a diffusion coefficient of $D_c = 1.42 \pm 0.14\,\text{cm}^2/\text{s}$. The net squared displacement of these paths (Fig. 1A) becomes a linear function of time after 2 s. *M. sanctus* ants therefore did indeed move according to Fickian diffusion in the arena centre (the $P1$-approximation holds).

The mean border following times (τ_q) are 7.82 ± 1.17 s for wall following, 5.91 ± 1.74 s for 6 cm obstacles, 2.48 ± 0.50 s for 4 cm obstacles and 3.31 ± 0.69 s for 2 cm obstacles. Note that these times result in border following

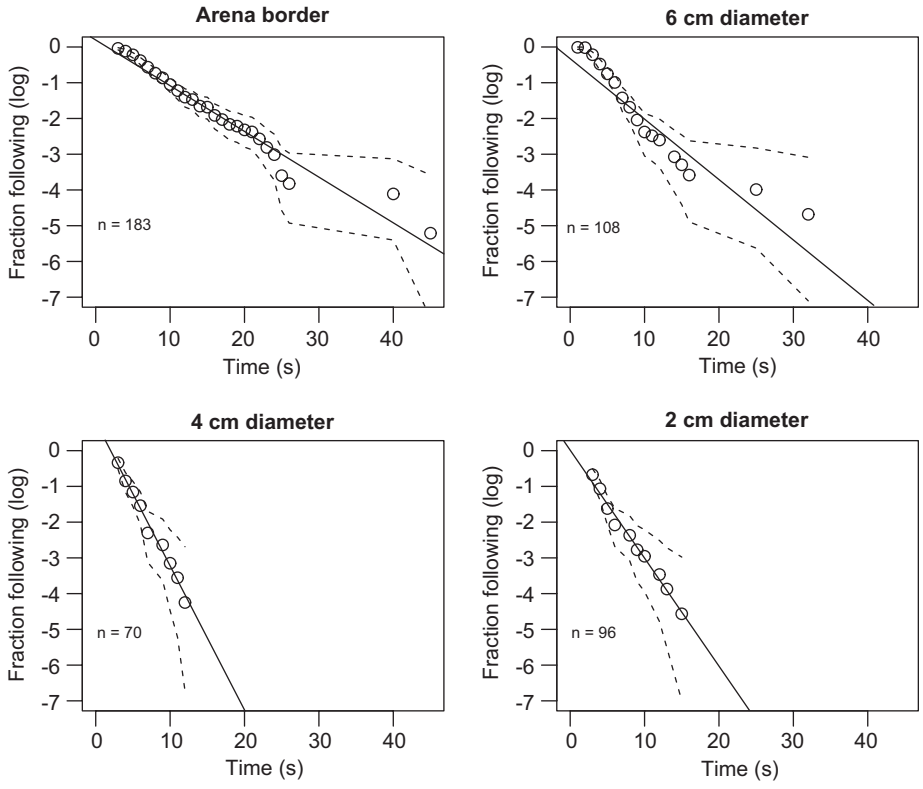

Fig. 3. Survival curves (Kaplan–Meier estimate, log-linear scale) of the border following times for borders of different curvatures. The dashed lines indicate the 95% confidence intervals, the straight line is the result of a weighted linear regression on the survival curve. All survival curves have an exponential distribution.

distances that are in all cases much longer than $2l$, a value we would expect if ants were to achieve a 2D random walk along the wall and simply continue walking straight ahead if the turning angle made them turn towards the wall. *M. sanctus* ants therefore show indeed thigmotactic behaviour. There was a significant effect of obstacle curvature on these times (Kruskal–Wallis test, $\chi^2 = 135.33$, $df = 3$, $p < 10^{-3}$). The border following times decreased with decreasing obstacle diameter (Fig. 2). The survival curves of the border following times (Fig. 3) show that the individual times were distributed exponentially for wall as well as for circular obstacles following. This result confirms the model hypothesis (see Section 2) that border following can be modelled as a Markovian process with a constant rate to quit the border. The mean wall following time before making a U-turn (τ_b) is 31.5 ± 4.1 s. Combined with ant speed v and the mean wall following time before quitting it (τ_q) we obtain the diffusion coefficient along the arena wall $D_b = 10.2 \pm 1.3\,\mathrm{cm}^2/\mathrm{s}$.

These mean wall following distances are of the same order of magnitude as the arena size. This raises the question whether the diffusion approximation (Appendix A) is appropriate for the non-stationary dynamics. To answer this question we can make numerical simulations with either Fickian diffusion or the telegraph equation (which does not make the diffusion approximation). For the telegraph equation we used the same numerical scheme as for Fickian diffusion, but with the flux density on the border implemented as an additional state variable according to Eq. (12). Fig. 1B shows that the dynamics of the two systems are practically the same, Fickian diffusion is therefore a reasonably good approximation of ant displacement along the border also during the non-stationary dynamics.

The spatio-temporal dynamics of models (3)–(5) with the parameter values estimated from the experiments and for the case of the empty arena are shown in Fig. 4. In the beginning the density equivalent to 40 ants is placed in the centre of the arena (where the real ants enter). These ants immediately start to diffuse (Fig. 4A) and reach the border within the first 20 s (Fig. 4F). Stationary state is reached after 5 min (Figs. 4D,H and 1B)). The 30 min allowed to reach this state in the real experiments are therefore largely sufficient.

The mean following times predicted by the model from the measured ant densities (Eq. (7)) and the times measured directly from individual ant movement show the same trend (Fig. 2). There is therefore a qualitative validation of the model prediction at stationary state. In the case of arena walls or large obstacles (6 cm) the predicted ranges also show some overlap with the 95% confidence interval of the border following times measured directly. However, this overlap disappears for smaller obstacles. This quantitative difference shows up qualitatively in the density plots (Fig. 5): while in the first case (no obstacles or large ones, Fig. 5A,B) ant density outside the border areas looks rather homogeneous (besides some increased density around the entry hole), distinct high density "routes" can be identified for smaller obstacles (Fig. 5C,D). These areas might arise for several reasons: (a) the obstacles channel the moving ants, (b) ants memorize routes with obstacles as landmarks or (c) ants mark their path by pheromones that guide other ants. In order to test these hypotheses we made an additional experiment with seven obstacles of 4 cm diameter and let it run for 2 h (analysing the densities during the last 90 min as above). We then removed the

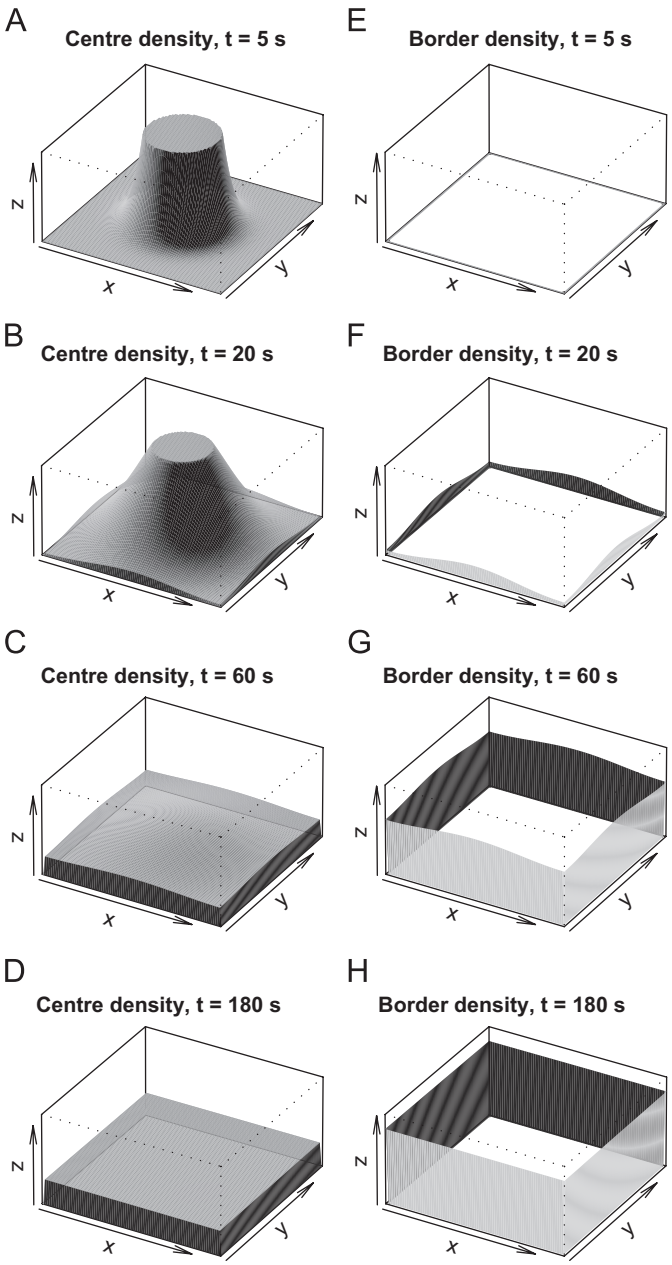

Fig. 4. Numerical simulation of Eqs. (3)–(5). Forty ants are released at time 0 in the centre of the arena. The left figures (A)–(D) show the spatio-temporal evolution of ant density in the centre of the arena, the right figures (E)–(H) that on the border (centre set to 0 in these figures). The height of the z-axis is fixed to the same value to permit comparison along time. Parameter values are $D_c = 0.00014\,\mathrm{m}^2/\mathrm{s}$, $D_b = 0.0010\,\mathrm{m}^2/\mathrm{s}$, $v_c = v_b = 0.014\,\mathrm{m/s}$, $\lambda_b = 0.11\,\mathrm{m}$ and the simulation was done on a 100 by 100 square grid with $\mathrm{d}x = \mathrm{d}y = 0.0035\,\mathrm{m}$ and $\mathrm{d}t = 0.002\,\mathrm{s}$.

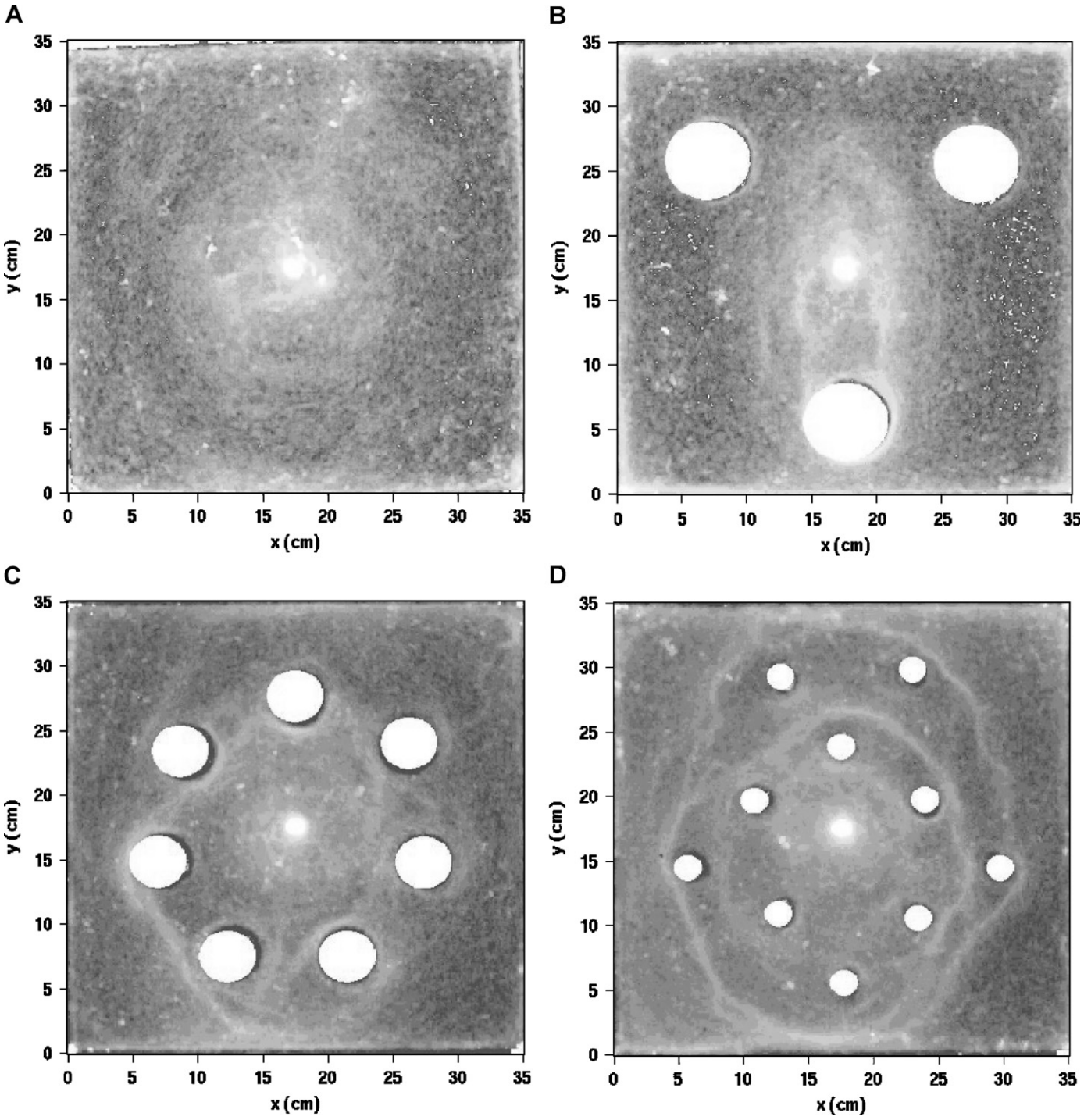

Fig. 5. Examples of the experimental mean density of ants (averaged over 90 min, high density indicated by white, low density by dark grey) observed in an empty arena (A), with three large obstacles (6 cm diameter, B), seven median obstacles (4 cm, C) or 10 small obstacles (2 cm, D).

obstacles and analysed ant displacement during another 90 min. The result (Fig. 6) was clear: the ants follow exactly the same routes. Since there are no more obstacles or landmarks ants must follow a pheromone trail.

5. Discussion

In this paper we pursue two objectives: (1) the rigorous derivation and validation of a model of ant displacement in 2D space with 1D borders, and (2) to use the stationary state predictions of this model to test whether the simultaneous displacement of many ants is "simply" the sum of the individual displacements.

Concerning the first objective our analysis confirms that the displacement of a single *M. sanctus* ant in a homogeneous 2D environment can be modelled as a correlated random walk (Challet et al., 2005). Such correlated random walks are common for many insects

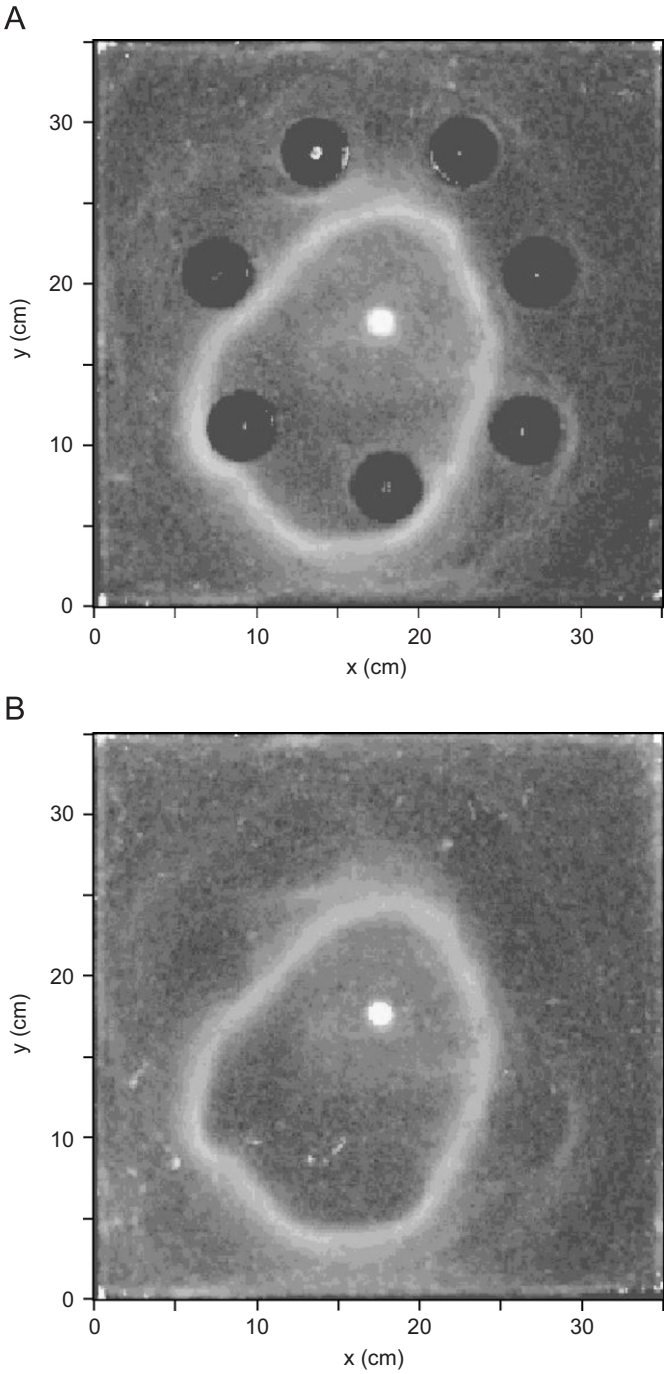

Fig. 6. Mean ant densities before (A) and after (B) removal of seven median obstacles (4 cm diameter). Ants clearly continue to follow the same (white) trail.

(Kareiva and Shigesada, 1983; Jeanson et al., 2003). These ants can be assumed to detect walls from a distance of 1 cm. If an ant were to use the same kind of correlated random walk along a wall and simply continue to move straight ahead when it is blocked by the wall we would expect a wall following distance approximately equal to twice the mean free path in the centre. The measured mean wall following distance was much above this value, showing unambiguously that the ants did have a thigmotactic behaviour. Such thigmotactic behaviour has been reported in several species of insects and investigated from a behavioural (Creed and Miller, 1990; Sikora et al., 1992; Camhi and Johnson, 1999; Dussutour et al., 2005) and from a physiological point of view (Cowan et al., 2006). We further showed that the rate to leave the border increased with higher curvature (more concave borders), exactly as Creed and Miller (1990) have observed for the American cockroach *Periplaneta americana* L. For a given curvature, however, the rate to leave the border remained constant (a homogeneous Markov process). Jeanson et al. (2003) have shown this Markov property for thigmotactic behaviour of first instar larvae of the German cockroach. Here we confirm and characterize this type of thigmotactic behaviour for the ant *M. sanctus*.

The description of insect displacement as a combination of a correlated random walk and thigmotactism with the Markov property is sufficient to create an IBM of animal movement. Here we go a step further by applying a mesoscopic approach to this IBM in order to derive continuous PDE of the diffusion type that permit to describe animal densities in a bounded space. All the approximations made in this derivation (diffusion and $P1$ approximation) have been validated for the case of *M. sanctus* exploratory behaviour.

Such a rigorously validated PDE model of ant displacement is a good starting point to study more complex spatial phenomena such as the object clustering reported in Jost et al. (2007). In the context of foraging *M. sanctus* ants are also known to create and move along pheromone trails (Jackson et al., 1989; Grasso et al., 1998, 1999), but no such collective behaviour has been reported for exploratory behaviour (though experiments in Fourcassié et al., 2003 suggest its existence). The predictions of our model should therefore also hold when many ants explore space simultaneously. We use in particular the prediction that the ratio of border over centre ant density at stationary state only depends on the thigmotactic component. Numerical simulations of the PDE show that this stationary state is reached within a couple of minutes. Testing this prediction with *M. sanctus* we show that it holds rather well in the case of an empty arena or if there are only few large obstacles. However, in the presence of strong heterogeneities in the form of many small obstacles the prediction breaks down and we demonstrate that ants lay and follow pheromone trails. A collective displacement mode is thus emerging. Further experimental work is required to identify the stimuli that trigger trail laying behaviour in *M. sanctus* ants. Pheromone marking might also occur permanently during exploratory displacement. In this case, if the ant movement is channelled by the obstacles, the ant density could increase sufficiently to create a persistent pheromone trail.

Habitat fragmentation increasingly leads to a mosaic landscape where animals are confronted with an alternation of borders and open space. Animal displacement in such heterogeneous environments is at the core of many

questions in ecology (e.g. Turchin, 1991; Johnson et al., 1992; Fagan et al., 1999; With et al., 1999; Ovaskainen and Cornell, 2003; Morales et al., 2005) and individual behaviour provides essential information to understand processes at the landscape level (Morales and Ellner, 2002). The mesoscopic approach provides a way on how to scale up from the individual to the population level in landscape ecology studies. The resulting PDE models are accessible to various non-linear analyses that permit to study phenomena on the system level while still being well-grounded in the individual statistical behaviour. They may thus be particularly useful in conservation biology to understand population level responses to landscape change.

Acknowledgements

We thank two anonymous reviewers for their critical but constructive comments. This work was supported by a grant from the interdisciplinary CNRS program ''Complexité du Vivant''.

Appendix A. The mesoscopic derivation of the diffusion equation

Though it is commonly known that (correlated) random walks can be described at the population level by diffusion equations, the underlying mathematics are not always accessible to the general biological reader, in particular the link between the diffusion coefficient and the individual movement parameters. This situation is complicated by the variety of notations and names used in the literature. To clarify the approach used in the present paper we will show here how the diffusion equation emerges from the individual movement behaviour. More formal developments can be found in Patlak (1953, ecological context) and Case and Zweifel (1967, statistical mechanics). This development will also highlight the underlying approximations and permit us to discuss their pertinence in the analysed experiments. The resulting model is therefore well-grounded in the underlying statistical individual behaviour and not simply an empirical PDE model.

A.1. From the pure transport equation to the mesoscopic model

Let $f = f(\vec{r}, \vec{u}, t)$ be the density of ants at time t and at the position $\vec{r}$ that move in direction $\vec{u}$ (the so-called distribution function in statistical physics). $\vec{r}$ and $\vec{u}$ are vectors in R^d, with $d = 1, 2$ or 3. We will first derive the transport equation in a heuristic way.

If the ants move at constant speed v in direction $\vec{u}$ and do not change direction we get the equation

$$f(\vec{r}, \vec{u}, t) = f(\vec{r} + v\vec{u}\,\mathrm{d}t, \vec{u}, t + \mathrm{d}t). \tag{8}$$

Or, making a Taylor expansion of the right side of Eq. (8) and still considering only ants moving in direction $\vec{u}$ gives

$$f(\vec{r} + v\vec{u}\,\mathrm{d}t, \vec{u}, t + \mathrm{d}t) \approx f(\vec{r}, \vec{u}, t) + \frac{\partial f}{\partial t}\,\mathrm{d}t + \frac{\partial f}{\partial \vec{r}} \cdot \frac{\partial \vec{r}}{\partial t}\,\mathrm{d}t. \tag{9}$$

Combining Eqs. (8) and (9) and using that $\partial f/\partial \vec{r} = \mathbf{grad}\, f$, $\partial \vec{r}/\partial t = v\vec{u}$ results in

$$\begin{aligned} 0 &= f(\vec{r} + v\vec{u}\,\mathrm{d}t, \vec{u}, t + \mathrm{d}t) - f(\vec{r}, \vec{u}, t) \\ &\approx \frac{\partial f}{\partial t}\,\mathrm{d}t + v\vec{u} \cdot \mathbf{grad}\, f\,\mathrm{d}t \end{aligned}$$

$$\Longrightarrow\ 0 \approx \frac{\partial f}{\partial t} + v\vec{u} \cdot \mathbf{grad}\, f$$

(where **grad** is the gradient operator). This is the transport equation that we will put on the left side of the mesoscopic equation, while we add on the right all the terms where ants join or quit $f(\vec{r}, \vec{u}, t)$,

$$\begin{aligned} \frac{\partial f}{\partial t} + v\vec{u} \cdot \mathbf{grad}\, f = &\int_{\vec{u}'} \frac{1}{\tau_b}\omega(\vec{u}|\vec{u}')f'\,\mathrm{d}\vec{u}' \\ &- \int_{\vec{u}'} \frac{1}{\tau_b}\omega(\vec{u}'|\vec{u})f\,\mathrm{d}\vec{u}' - \frac{1}{\tau_q}f, \end{aligned} \tag{10}$$

where the first part represents the ants currently moving in direction $\vec{u}'$ that change their direction to $\vec{u}$, the second part considers those who change their direction from $\vec{u}$ to $\vec{u}'$ and the third those that are lost from the system (this term will account for the ants quitting the border and returning to the centre). f' simply denotes $f(\vec{r}, \vec{u}', t)$. τ_b is the mean time walking straight ahead before turning, and $\omega(\vec{u}|\vec{u}')$ is the probability density function that an ant moving in direction $\vec{u}'$ will change to direction $\vec{u}$ (also called the phase function). We assume that turning happens at a constant rate and only depends on the cosine between $\vec{u}$ and $\vec{u}'$,

$$\omega(\vec{u}|\vec{u}') \equiv \omega(\vec{u} \cdot \vec{u}').$$

Until here no approximations were made, we only translated the exponential features of the individual statistical behaviour (observed in Fig. 3) in terms of the distribution function f.

A.2. The passage to the macroscopic model

We now want to derive the corresponding equations for the macroscopic variables, local ant density $n(\vec{r}, t) = \int_{\vec{u}} f(\vec{r}, \vec{u}, t)\,\mathrm{d}\vec{u}$ and the flux density vector $\vec{j}(\vec{r}, t) = \int_{\vec{u}} vf(\vec{r}, \vec{u}, t)\vec{u}\,\mathrm{d}\vec{u}$. Doing so we will have to make assumptions to get rid of the directional character of the distribution function (passage from the mesoscopic to the macroscopic description).

For the local ant density we simply integrate Eq. (10) over all directions $\vec{u}$. The algebra for the transport term is

quite straightforward,

$$\int_{\vec{u}}\left(\frac{\partial f}{\partial t}+v\vec{u}\cdot\mathbf{grad}f\right)\mathrm{d}\vec{u}=\int_{u}\frac{\partial f}{\partial t}\,\mathrm{d}\vec{u}+v\int_{\vec{u}}\vec{u}\cdot\mathbf{grad}f\,\mathrm{d}\vec{u}$$
$$=\frac{\partial n}{\partial t}+v\,\mathbf{div}\int_{\vec{u}}f\vec{u}\,\mathrm{d}\vec{u}=\frac{\partial n}{\partial t}+\mathbf{div}\vec{j}$$

with **div** being the divergence operator.

The integration of the right side of Eq. (10) is also straightforward, we get

$$\int_{\vec{u}}\int_{\vec{u}'}\frac{\omega(\vec{u}'\cdot\vec{u})}{\tau_b}f\,\mathrm{d}\vec{u}'\,\mathrm{d}\vec{u}=\int_{\vec{u}}\frac{f}{\tau_b}\underbrace{\int_{\vec{u}'}\omega(\vec{u}'\cdot\vec{u})\,\mathrm{d}\vec{u}'}_{=1}\,\mathrm{d}\vec{u}=\frac{n}{\tau_b},$$

$$\int_{\vec{u}}\int_{\vec{u}'}\frac{\omega(\vec{u}\cdot\vec{u}')}{\tau_b}f'\,\mathrm{d}\vec{u}'\,\mathrm{d}\vec{u}=\frac{1}{\tau_b}\int_{\vec{u}'}f'\underbrace{\int_{\vec{u}}\omega(\vec{u}\cdot\vec{u}')\,\mathrm{d}\vec{u}}_{=1}\,\mathrm{d}\vec{u}'=\frac{n}{\tau_b},$$

$$\int_{\vec{u}}\frac{1}{\tau_q}f\,\mathrm{d}\vec{u}=\frac{n}{\tau_q}.$$

In sum, we get the macroscopic equation

$$\frac{\partial n}{\partial t}+\mathbf{div}\,\vec{j}=\frac{n}{\tau_b}-\frac{n}{\tau_b}-\frac{n}{\tau_q}=-\frac{n}{\tau_q}. \tag{11}$$

To get the macroscopic equation for the flux we simply multiply Eq. (10) by $\vec{u}$ before integrating over all $\vec{u}$,

$$\int_{\vec{u}}\left(\frac{\partial f}{\partial t}\vec{u}+v\vec{u}\cdot\mathbf{grad}f\vec{u}\right)\mathrm{d}\vec{u}=\int_{\vec{u}}\int_{\vec{u}'}\omega(\vec{u}|\vec{u}')f'\vec{u}\,\mathrm{d}\vec{u}'\,\mathrm{d}\vec{u}$$
$$-\int_{\vec{u}}\int_{\vec{u}'}\omega(\vec{u}'|\vec{u})f\vec{u}\,\mathrm{d}\vec{u}'\,\mathrm{d}\vec{u}$$
$$-\int_{\vec{u}}\frac{1}{\tau_q}f\vec{u}\,\mathrm{d}\vec{u}.$$

While the right side is also straightforward to integrate, the left side is slightly more complicated (not detailed here, see for example Case and Zweifel, 1967). The result is the equation

$$\frac{\partial\vec{j}}{\partial t}+\frac{v^2}{d}\mathbf{grad}\,n\approx\left((g-1)\frac{1}{\tau_b}-\frac{1}{\tau_q}\right)\vec{j} \tag{12}$$

with $g=\int_{\vec{u}'}(\vec{u}'\cdot\vec{u})\omega(\vec{u}'\cdot\vec{u})\,\mathrm{d}\vec{u}'$ being the mean cosine of the phase function. Note that this equation is exact only for $d=1$. In higher dimensions one must make the so-called $P1$-approximation (Case and Zweifel, 1967). The name $P1$ means that in 3D or 2D only the first two terms of the spherical harmonic decomposition or the Fourier series are kept, respectively. If this $P1$-approximation did not hold then the mean net squared displaced of animals (Fig. 1) would no longer become a linear function of time.

A.3. Application to the experimental system

Since the measured mean free paths in our experimental system are much smaller than the arena dimension we can make the diffusion approximation (stationary assumption for the flux density, $\partial\vec{j}/\partial t=0$), Eq. (12) therefore yields $\vec{j}=-(v^2/d((1-g)/\tau_b+1/\tau_q))\,\mathbf{grad}\,n$ that we can plug into Eq. (11),

$$\frac{\partial n}{\partial t}=-\mathbf{div}\,\vec{j}=\frac{v^2}{d((1-g)/\tau_b+1/\tau_q)}\mathbf{div}\,\mathbf{grad}\,n$$
$$=\frac{v^2}{d((1-g)/\tau_b+1/\tau_q)}\Delta n.$$

This is standard Fickian diffusion with a diffusion coefficient

$$D=\frac{v^2}{d((1-g)/\tau_b+1/\tau_q)}.$$

In the arena centre ($d=2$) no ants disappear (that is, there is no term involving τ_q) and τ_b is the mean free path l divided by ant speed v,

$$D_c=\frac{v^2}{2(1-g)v/l}=\frac{vl}{2(1-g)}.$$

Along the border ($d=1$) τ_q corresponds to the mean time of border following before returning to the centre area and τ_b is the mean time before making a U-turn. The phase function is in this case a discrete probability function with value 1 in case of a U-turn ($\vec{u}\cdot\vec{u}'=-1$) and value 0 for continuing in the same direction ($\vec{u}\cdot\vec{u}'=1$), we therefore get $g=-1$ and the diffusion coefficient becomes

$$D_b=\frac{v^2}{2/\tau_b+1/\tau_q}.$$

Note that without the diffusion approximation we would simply get the telegraph equation. The stationary state predictions are not changed by this approximation, but the non-stationary dynamics are affected. In our system the mean wall following distances are long compared to the arena size, it is therefore useful to test the effect on non-stationary dynamics by numerical simulations.

References

Benhamou, S., 2004. On the expected net displacement of animals' random movements. Ecol. Modelling 171, 207–208.

Bovet, P., Benhamou, S., 1988. Spatial analysis of animals' movements using a correlated random walk model. J. Theor. Biol. 131, 419–433.

Camazine, S., Deneubourg, J.-L., Franks, N.R., Sneyd, J., Theraulaz, G., Bonabeau, E., 2001. Self-organization in Biological Systems. Princeton University Press, Princeton.

Camhi, J.M., Johnson, E.N., 1999. High-frequency steering maneuvers mediated by tactile cues: antennal wall-following in the cockroach. J. Exp. Biol. 202, 631–643.

Case, K., Zweifel, P., 1967. Linear Transport Theory. Addison-Wesley, New York, USA.

Challet, M., Jost, C., Grimal, A., Lluc, J., Theraulaz, G., 2005. How temperature influences displacements and corpses aggregation behaviors in the ant *Messor sancta*. Insectes Soc. 52, 305–315.

Cowan, N.J., Lee, J., Full, R.J., 2006. Task-level control of rapid wall following in the American cockroach. J. Exp. Biol. 209, 1617–1629.

Creed Jr., R.P., Miller, J.R., 1990. Interpreting animal wall-following behavior. Experientia 46, 758–761.

Dussutour, A., Deneubourg, J.-L., Fourcassié, V., 2005. Amplification of individual preferences in a social context: the case of wall-following in ants. Proc. R. Soc. London B 272, 705–714.

Einstein, A., 1905. Über die von der molekularkinetischen Theorie der Wärme geforderte Bewegung von in ruhenden Flüssigkeiten suspendierten Teilchen. Ann. Phys. 17, 549–560.

Fagan, W.F., Cantrell, R.S., Cosner, C., 1999. How habitat edges change species interactions. Am. Nat. 153 (2), 165–182.

Faugeras, B., Maury, O., 2007. Modeling fish population movements: from an individual-based representation to an advection–diffusion equation. J. Theor. Biol. 247, 837–848.

Fourcassié, V., Bredard, C., Volpatti, K., Theraulaz, G., 2003. Dispersion movements in ants: spatial structuring and density-dependent effects. Behav. Processes 63, 33–43.

Fraenkel, G.S., Gunn, D.L., 1961. The Orientation of Animals: Kineses, Taxes and Compass Reactions. Dover Publications, Inc., New York.

Grasso, D.A., Mori, A., Le Moli, F., 1998. Chemical communication during foraging in the harvesting and *Messor capitatus* (Hymenoptera, Formicidae). Insectes Soc. 45, 85–96.

Grasso, D.A., Mori, A., Le Moli, F., 1999. Recruitment and trail communication in two species of *Messor* ants (Hymenoptera, Formicidae). Ital. J. Zool. 66, 373–378.

Grimm, V., Railsback, S.F., 2005. Individual-based Modeling and Ecology. Princeton University Press, Princeton.

Grünbaum, D., 1999. Advection–diffusion equations for generalized tactic searching behaviors. J. Math. Biol. 38, 169–194.

Haccou, P., Meelis, E., 1992. Statistical Analysis of Behavioural Data: An Approach Based on Time Structured Models. Oxford University Press, Oxford.

Jackson, B.D., Wright, P.J., Morgan, D.E., 1989. 3-Ethyl-2,5-dimethylpyrazine, a component of the trail pheromone of the ant *Messor bouvieri*. Experientia 45, 487–489.

Jeanson, R., Blanco, S., Fournier, R., Deneubourg, J.-L., Fourcassié, V., Theraulaz, G., 2003. A model of animal movements in a bounded space. J. Theor. Biol. 225, 443–451.

Jeanson, R., Rivault, C., Deneubourg, J.-L., Blanco, S., Fournier, R., Jost, C., Theraulaz, G., 2005. Self-organised aggregation in cockroaches. Anim. Behav. 69, 169–180.

Johnson, C.J., Wiens, J.A., Milne, B.T., Crist, T.O., 1992. Animal movements and population dynamics in heterogeneous landscapes. Landscape Ecol. 7, 63–75.

Jost, C., Verret, J., Casellas, E., Gautrais, J., Challet, M., Lluc, J., Blanco, S., Clifton, M., Theraulaz, G., 2007. The interplay between a self-organized process and an environmental template: corpse clustering under the influence of air currents in ants. J. R. Soc. Interface 4, 107–116.

Kareiva, P.M., Shigesada, N., 1983. Analyzing insect movement as a correlated random walk. Oecologia 56, 234–238.

Morales, J.M., Ellner, S.P., 2002. Scaling up animal movements in heterogeneous landscapes: the importance of behavior. Ecology 83, 2240–2247.

Morales, J.M., Fortin, D., Frair, J., Merrill, E.H., 2005. Adaptive models for large herbivore movements in heterogeneous landscapes. Landscape Ecol. 20, 301–316.

Okubo, A., Levin, S.A., 2001. Diffusion and Ecological Problems: Modern Perspectives, second ed. Springer, New York.

Ovaskainen, O., Cornell, S.J., 2003. Biased movement at a boundary and conditional occupancy times for diffusion processes. J. Appl. Probab. 40, 557–580.

Parrish, J.K., Hamner, W.M. (Eds.), 1997. Animal Groups in Three Dimensions. Cambridge University Press, London.

Patlak, C.S., 1953. Random walk with persistence and external bias. Bull. Math. Biophys. 15, 311–338.

Press, W.H., Teukolsky, S.A., Vetterling, W.T., Flannery, B.P., 1992. Numerical Recipes in C: The Art of Scientific Computing, second ed. Cambridge University Press, London.

Sikora, J., Baranowski, Z., Zajaczkowska, M., 1992. Two-state model of *Paramecium bursaria* thigmotaxis. Experientia 48, 789–792.

Theraulaz, G., Bonabeau, E., Nicolis, S.C., Solé, R.V., Fourcassié, V., Blanco, S., Fournier, R., Joly, J.-L., Fernández, P., Grimal, A., Dalle, P., Deneubourg, J.-L., 2002. Spatial patterns in ant colonies. Proc. Natl Acad. Sci. USA 99 (15), 9645–9649.

Tourtellot, M.K., Collins, R.D., Bell, W.J., 1991. The problem of movelength and turn definition in analysis of orientation data. J. Theor. Biol. 150, 287–297.

Turchin, P., 1991. Translating foraging movements in heterogeneous environments into the spatial distribution of foragers. Ecology 72, 1253–1266.

Turchin, P., 1998. Quantitative Analysis of Movement: Measuring and Modeling Population Redistribution in Animals and Plants. Sinauer Associates, Sunderland, MA.

With, K.A., Cadaret, S.J., Davis, C., 1999. Movement responses to patch structure in experimental fractal landscapes. Ecology 80, 1340–1353.

Zar, J.H., 1999. Biostatistical Analysis, fourth ed. Prentice-Hall, New Jersey.